

“Zeoball” $[\text{Sn}_{36}\text{Ge}_{24}\text{Se}_{132}]^{24-}$: A Molecular Anion with Zeolite-Related Composition and Spherical Shape

Yumei Lin, Werner Massa, and Stefanie Dehnen*

Fachbereich Chemie and Wissenschaftliches Zentrum für Materialwissenschaften, Philipps-Universität Marburg, Hans-Meerwein-Straße, D-35032 Marburg, Germany

S Supporting Information

ABSTRACT: Ionothermal reactions of $[\text{Ge}_4\text{Se}_{10}]^{4-}$ with $\text{SnCl}_4 \cdot 5\text{H}_2\text{O}$ yielded $[\text{BMMIm}]_{24}[\text{Sn}_{36}\text{Ge}_{24}\text{Se}_{132}]$ (**ZBT-1**) and $[\text{BMIm}]_{24}[\text{Sn}_{32.5}\text{Ge}_{27.5}\text{Se}_{132}]$ (**ZBT-2**; B(M)MIm = 1-butyl-(2,)-3-(di)methylimidazolium]. These contain the largest known discrete polyanion consisting only of main-group elements. In spite of a zeolite-related composition, the 192-atom “zeoball” anion adopts a spherical shape, which has been unprecedented in the chemistry of zeolites and their homologues and relatives. Preliminary studies indicated that **ZBT-1** traps I_2 molecules and induces heterolytic I–I bond cleavage.

Microporous materials based on zeolites with well-defined structures have widespread applications, such as in separation, cation exchange, and petroleum processing.¹ The continuously increasing demands for porous materials with highly specific properties and applications have inspired scientists to develop new strategies for obtaining such compounds.² Since the excellent performance of zeolite materials is essentially determined by their structural characteristics which is further related to their composition, the synthesis of new zeolite materials has been significantly advanced during the last several years.^{3,4a} Hence, replacement of the framework O^{2-} anions with S^{2-} or Se^{2-} and/or the substitution of different transition or main-group metal atoms for Si or Al has allowed for the generation of an even greater variety of fascinating structures—including coordination geometries other than tetrahedral—with additional, tunable properties such as optoelectronic characteristics, photocatalytic properties, fast-ion conductivity, and molecular trapping capabilities.^{4,5}

Besides classical hydrothermal/solvothermal methods, increasing activity has become noticeable in the employment of ionothermal reactions in the synthesis of zeolites,⁶ metal–organic frameworks,⁷ and nanomaterials.⁸ This is due to the excellent solvating properties of ionic liquids (ILs), such as negligible vapor pressure, high thermal stability, wide liquidus range, and the ability to dissolve a variety of materials. Nevertheless, the application of this technique for the preparation of chalcogenides has not been extensively explored.⁹

We have recently extended our bottom-up strategy for the synthesis of microporous chalcogenides by using approved binary precursors containing $[\text{ME}_4]$ units (M = main-group or transition metal atom; E = chalcogen atom)¹⁰ in the new solvent environment of ILs. In a preliminary study, we

investigated the treatment of the chalcogenidostannate phase $[\text{K}_4(\text{H}_2\text{O})_4][\text{SnSe}_4]$, containing the binary precursor $[\text{SnSe}_4]^{4-}$, with the IL $[\text{BMIm}]\text{BF}_4$ (BMIm = 1-butyl-3-methylimidazolium, $\text{C}_8\text{H}_{15}\text{N}_2$), which led to the formation of the unique 3D open-framework selenidostannate $[\text{BMIm}]_4[\text{Sn}_9\text{Se}_{20}]$.¹¹

A new expansion of this strategy that used a larger precursor unit, $[\text{Ge}_4\text{Se}_{10}]^{4-}$, and introduced another metal component, $\text{SnCl}_4 \cdot 5\text{H}_2\text{O}$, with the aim of obtaining a ternary porous chalcogenide was successful in the preparation of two novel compounds, $[\text{BMMIm}]_{24}[\text{Sn}_{36}\text{Ge}_{24}\text{Se}_{132}]$ (**ZBT-1**; BMMIm = 1-butyl-2,3-dimethylimidazolium, $\text{C}_9\text{H}_{17}\text{N}_2$) and $[\text{BMIm}]_{24}[\text{Sn}_{32.5}\text{Ge}_{27.5}\text{Se}_{132}]$ (**ZBT-2**). These were synthesized by heating $[\text{K}_4(\text{H}_2\text{O})_3][\text{Ge}_4\text{Se}_{10}]$ (56 mg, 0.043 mmol) and $\text{SnCl}_4 \cdot 5\text{H}_2\text{O}$ (40 mg, 0.11 mmol) in $[\text{BMMIm}][\text{BF}_4]$ (0.5 g) or $[\text{BMIm}][\text{BF}_4]$ (0.5 mL), respectively, in the presence of a small amount of 2,6-dimethylmorpholine (DMMP, 0.05 mL) in a sealed pyrex tube (~10 mL capacity) at 150 °C for 2 days. Upon cooling to room temperature, air-stable, red block crystals were obtained by filtration, washed several times with deionized water and ethanol, and dried under air (yields: **ZBT-1**, 21 mg, 34% with respect to Sn; **ZBT-2**, 17 mg, 28% with respect to Sn). Although the title compounds possess zeolite-related compositions, according to $\text{A}_x[\text{M}_x\text{E}^{14}_y\text{E}^{16}_z]$ (A = cation; M = metal ion; E^{14} = group-14 element = tetrel; E^{16} = group-16 element = chalcogen), they comprise discrete, molecular anions with a spherical shape and a large spherical cavity, which additionally represent the largest known discrete cluster consisting only of atoms of heavy main-group elements (Figure 1).

On the basis of the zeolite-related composition that uniquely meets a spherical shape in the anionic units described here, we would like to introduce the latter as “zeoballs” and the new class of compounds as “zeoball” tetrelate (**ZBT**) phases.

The crystal structures of **ZBT-1** and **ZBT-2** were determined by means of single-crystal X-ray diffraction (XRD), which also helped to attribute the slight differences between the two anionic formulas to partial Ge/Sn disorder [see the Supporting Information (SI)]. Both compounds comprise macroanionic units $[\text{Sn}_{36-x}\text{Ge}_{24+x}\text{Se}_{132}]^{24-}$ (Figure 1), with $x = 0$ for **ZBT-1** and 3.5 for **ZBT-2**. Besides the partial disorder, the anionic structures differ only marginally. The following discussion of the anionic structure and all of the figures will refer to the $x = 0$ case, as actually found for **ZBT-1** and as idealized for **ZBT-2** if the disorder is disregarded. Charge neutrality is achieved by the

Received: December 11, 2011

Published: February 27, 2012



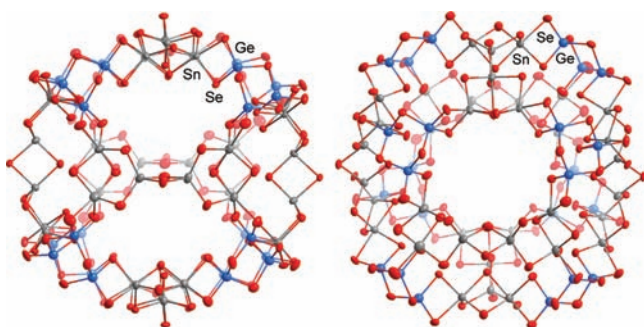


Figure 1. Two different orientations of the $[\text{Sn}_{36}\text{Ge}_{24}\text{Se}_{132}]^{24-}$ anionic structure of the title compounds, disregarding partial Sn/Ge disorder.

inclusion of 24 counteranions, $[\text{BMMIm}]^+$ in **ZBT-1** and $[\text{BMIm}]^+$ in **ZBT-2**, that are arranged inside and outside the anions and are packed according to distorted versions of the face-centered cubic (fcc) type in the crystal structure (see Figures S5 and S7 in the SI).

The polyanion exhibits an outer diameter of 2.83 nm, including van der Waals radii of the surface atoms, and comprises 192 atoms that approach a highly symmetric and regular pattern, although the actual crystallographic symmetry is only C_i in both compounds. The architecture of the cluster is based on two secondary building units (SBUs; Figure 2a,b), a

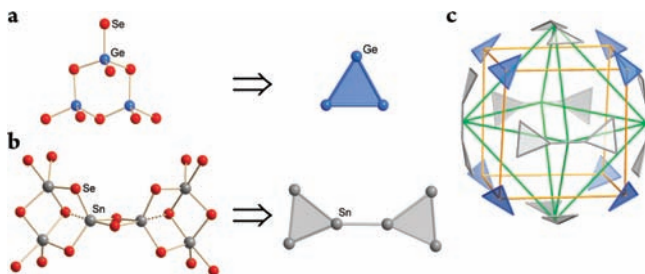


Figure 2. (a, b) Structures of the two SBUs in the title compounds along with their simplified representations: (a) $[\text{Ge}_3\text{Se}_9]$ (SBU-1); (b) $[\text{Sn}_6\text{Se}_{18}]$ (SBU-2). Dashed lines in SBU-2 represent two $\text{Sn}\cdots\text{Se}$ contacts above 2.8 Å that are shown to illustrate the structural relation of SBU-2 with two $[\text{Sn}_3\text{Se}_4(\mu\text{-Se})_6]$ semicubes linked by two $\mu\text{-Se}$ bridges. (c) Pseudo- T_h -symmetric arrangement of eight SBU-1 and six SBU-2 within the $[\text{Sn}_{36}\text{Ge}_{24}\text{Se}_{132}]^{24-}$ anion.

$[\text{Ge}_3\text{Se}_9]$ unit (SBU-1) and a $[\text{Sn}_6\text{Se}_{18}]$ unit (SBU-2) that are linked by sharing common Se atoms. SBU-1 represents a fragment of the supertetrahedral precursor anion $[\text{Ge}_4\text{Se}_{10}]^{4-}$ that is missing one $[\text{Ge}-\text{Se}]$ corner. As in the precursor, the Ge atoms are tetrahedrally surrounded by Se ligands, and the three $[\text{GeSe}_4]$ tetrahedra are corner-linked. SBU-2 comprises two $[\text{Sn}_3\text{Se}_4(\mu\text{-Se})_6]$ semicubes that are linked by sharing two $\mu\text{-Se}$ ligands; thus, it is related to the structure of the polymeric phase $\{[\text{Sn}_3\text{Se}_7]^{2-}\}_n$,¹² which represents a network of $[\text{Sn}_3\text{Se}_4(\mu\text{-Se})_6]$ semicubes linked via two $\mu\text{-Se}$ ligands per Sn atom. However, one of the $\text{Sn}\cdots\text{Se}$ contacts in each semicube is too long (>2.8 Å) to be considered to be a bond; therefore, unlike the situation in $\{[\text{Sn}_3\text{Se}_7]^{2-}\}_n$, only four of the six Sn atoms are five-coordinate with trigonal bipyramidal coordination geometry [$\text{Sn}-\text{Se}_{\text{eq}} = 2.533(3)\text{--}2.584(3)$ Å (average 2.558 Å) in **ZBT-1** (values of the less-disordered anion **1** only) and $2.521(4)\text{--}2.585(3)$ Å (average 2.554 Å) in **ZBT-2** (disregarding disordered Sn7); $\text{Sn}-\text{Se}_{\text{ax}} = 2.640(3)\text{--}2.787(3)$ Å (average

2.712 Å) in **ZBT-1** and $2.622(3)\text{--}2.837(3)$ Å (average 2.713 Å) in **ZBT-2**].

The remaining two Sn atoms in SBU-2 are tetrahedrally surrounded and share the two $\mu\text{-Se}$ atoms that connect the two semicubes; the observations reflect once more the higher structural flexibility of Sn atoms in comparison to Ge atoms and also indicate a clear discrepancy between the present phases and the so-called “zeotype” compounds, which are restricted on four-connected networks. To build up the anionic cluster, six SBU-2 fragments are arranged at the corners of an octahedron in a pseudo- T_h -symmetric fashion and are further linked by sharing two $\mu\text{-Se}$ ligands with eight SBU-1 fragments located at the corners of a cube to form the spherical structure (Figure 2c).

For a detailed analysis of the architecture of **ZBT-1** and **ZBT-2**, the cluster structure was simplified by representing the $[\text{Ge}_3]$ and $[\text{Sn}_3]$ units of SBU-1 and SBU-2, respectively, as individual triangles and regarding the bridging by two $\mu\text{-Se}$ units as a simple line. This way, one obtains a truncated dodecahedron in which the corners are cut off, thereby producing 12 decagonal faces and 20 triangular faces (Figure 3). When the $[\text{Ge}_3]$ and $[\text{Sn}_3]$ units are considered as single

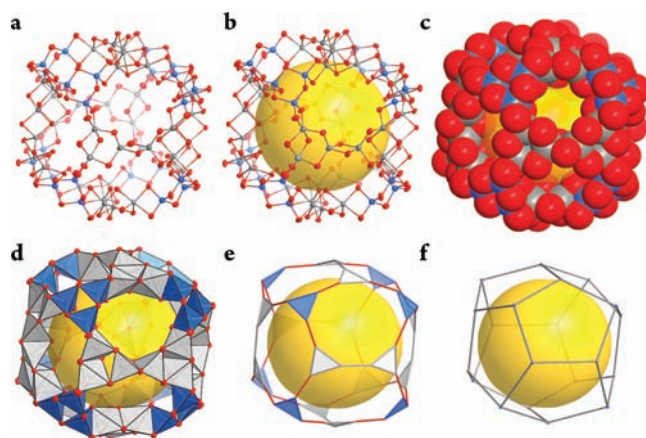


Figure 3. Analysis of the architecture of the $[\text{Sn}_{36}\text{Ge}_{24}\text{Se}_{132}]^{24-}$ anion. (a) The anionic structure shown in a slightly rotated orientation with respect to Figure 1. (b) The sphere inside the cavity has a diameter of 15.4 Å according to the smallest center-to-center distance of opposite Se atoms, which is reduced to 11.6 Å upon consideration of van der Waals radii. (c) Space-filling model illustrating the actual window opening with min/max diameters of 5.6/8.8 Å. (d, e) Simplification of the polyhedral representation into a truncated pentagonal dodecahedron with eight $[\text{Ge}_3]$ triangles (blue), 12 $[\text{Sn}_3]$ triangles (gray), and 12 decagonal faces. (f) Further simplification into a pentagonal dodecahedron upon reduction of the $[\text{Ge}_3]$ and $[\text{Sn}_3]$ units to single nodes.

nodes, the structure can be further simplified into a dodecahedron composed of 12 regular pentagonal faces and 20 vertices, according to the architecture of the smallest known fullerene cage, C_{20} . Fullerene-like inorganic clusters have attracted attention because of their high symmetry and molecular aesthetics, fascinating bonding features, and unusual properties.¹³ However, many of them possess multishell structures and hence are without large cavities or windows, inhibiting their application in many areas. In the title compounds, a large spherical cavity is accessible through 12 windows with open diameters of (min \times max) $5.6\text{--}6.2$ Å \times $7.9\text{--}8.8$ Å in **ZBT-1** and $5.7\text{--}6.3$ Å \times $7.7\text{--}8.7$ Å in **ZBT-2**.

The spherical body that fits inside the anion has a diameter of 11.6 Å under consideration of the van der Waals radii of the inner atoms, corresponding to an inner volume of 820 Å³. This is similar to the corresponding measure of the Faujasite supercage (14.1 Å) within the three-dimensional channel structure of the typical large-cage zeolite. In contrast to the recently reported ZIF-95 and ZIF-100, which exhibit extraordinarily huge cavities (24.0 and 35.6 Å for ZIF-95 and ZIF-100, respectively) but highly diminishing windows (largest apertures 3.65 and 3.35 Å, respectively) caused by organic groups being directed toward the opening of the cavities,¹⁴ the cavity of the ZBT anions is not blocked by covalently bonded ligands. Since the windows might enable a variety of further species to enter the cage, such clusters with a confined volume might act as nanoreactors or as nanomolds for calibrated and monodisperse nanomaterials.

The polyanion of the title compounds represents the largest known discrete cluster consisting only of atoms of heavy main-group elements, with regard to both its size and the number of atoms involved. Large, crystallographically defined chalcogenide clusters have attracted considerable interest because they behave like artificial atoms and thus are relevant to semiconductor nanoparticles as “quantum dots”.¹⁵ However, a significant increase in the negative charge with increasing cluster size inhibits the isolation of very large clusters. Feng and co-workers¹⁶ have shown that employing multiple charge-complementary metal cations allows for an effective reduction of the charge in a series of supertetrahedral T_n clusters. In the case of ZBT-1, the isolation of the extraordinarily large cluster was possible as a result of two factors that contribute to partial reduction of the negative charge: first, the presence of high-valence metal ions (i.e., Sn⁴⁺, Ge⁴⁺), and second, the formation of a sphere with a polymer-like, open atomic arrangement on a minimal surface (instead of the usually observed supertetrahedra, which rather represent fragments of dense solid-state phases and thus exhibit many negatively charged atoms on their plane faces). The second point is clearly attributed to the application of the other synthetic approach and its yet unexplored impact on the formation mechanism. Indeed, similar reactions of adamantane-type germanate anions [Ge₄E₁₀]⁴⁻ (E = S, Se) with various metal ions (e.g., Pt²⁺, Mn²⁺, Zn²⁺, Cd²⁺, Sb³⁺, Sn⁴⁺) in traditional solution procedures led to different, mesostructured materials.¹⁷ This emphasizes that the ionothermal method is a promising approach for the synthesis of new crystalline chalcogenides with unique structural and physical features that are inaccessible using well-established techniques. It should be noted that the presence of a small amount of amine is necessary in this reaction. The role of the amine is not yet completely clear; however, on the basis of the observation that conducting the same reaction in the absence of amine resulted in the formation of an uncharacterized Ge/Se-containing powder, whereas an excess of amine led to an unidentified microcrystalline Sn/Se phase, it is assumed that the amine subtly affects the assembly of the Sn/Se binary units. This assumption is confirmed by the fact that upon replacement of the reactant SnCl₄·5H₂O by the preformed precursor [K₄(H₂O)₄][SnSe₄], ZBT-2 was formed without the addition of amine; however, the crystal quality and yield were not as good as in the other case. The amine may also play a secondary role during the crystal growth. This phenomenon was explored for the formation of molecular sieves in ILs. According to these studies, a hydrogen-bonded hybrid of an imidazolium IL with an organic amine acts as the

structure-directing agent for the initial nucleation selectivity, whereas the imidazolium cations themselves act as the pore-filling agents in the crystal growth.¹⁸

In ZBT-2, 12 of the 24 counterions that compensate for the 24 negative charges of the anion in the crystal structure are arranged at the windows, with the imidazolium rings located near the centers of the windows and the butyl groups extending into the cavity. The remaining 12 cations surround the cages and are equally distributed for optimal charge compensation (Figures S3 and S6). The situation is similar but more complicated in ZBT-1, where two individual “zeoballs” are present and only 21 of the 24 symmetry-independent cations could be localized on the difference Fourier map.

An obvious question was whether the title compounds may contribute to the class of compounds with functional ball-like molecules, such as fullerenes, further organic spheres, or the spherical variants of polyoxometalates, so-called “Keplerates”.^{13,19} Since the counterions are not covalently bonded to the cages, and in agreement with the observation of disorder and thus high dynamic mobility of the organic groups (see the SI), small molecules or atoms might pass through. For preliminary studies of the molecular trapping capability and/or reactivity of the title compounds, we chose neutral I₂ molecules, which are of interest with respect to the role of the I⁻/I₃⁻ couple as redox species in electrolytes of dye-sensitized TiO₂ solar cells (DSSCs).²⁰ Accordingly, previous reports on the uptake of I₂ in framework cavities, heterolytic dissociation of I₂, or redox reactions that occur between the host and I₂ are available.²¹ I₂ was delivered both via the gas phase to solid ZBT-1 or via solution to suspensions of ZBT-1 [notably, both ZBT-1 and ZBT-2 are insoluble in all common solvents because of the extremely high charge of the anions, and they decompose into soluble selenidogermanate and selenidostannate fragments upon treatment with dimethyl sulfoxide (DMSO) or ethane-1,2-diamine (en)]. The study confirmed that the ZBT phase does not merely trap I₂ upon exposure of dry samples of ZBT-1 to I₂ vapor to form a loaded form, generally denoted as ZBT-1·nI₂, but it also strongly activates heterolytic I–I bond cleavage when liquor is present, while the “zeoball” cages stay intact. UV–vis spectra recorded upon soaking the loaded crystals in ethanol or water showed the presence of I₃⁻ and/or I⁻, respectively, indicating that both ZBT-1·n(I⁺⋯I⁻) and ZBT-1·n(I⁺⋯I₃⁻) are formed (Figure 4 and Figures S9 and S10). Depending on the absence or presence of solvent for the delivery of I₂ and on the nature of the solvent used, different observations were made (see the SI for more details).

The amount of I₂ to be taken up, and of I₃⁻ to be observed in the ethanol solution, is additionally dependent on the I₂ concentration of the cyclohexane solution. Thus, upon trapping of larger amounts of I₂, the sample first releases I⁻, which is then partially consumed by I₂ to form increasing amounts of I₃⁻ as time goes by (Figure 4b). Decreasing amounts of I₂ in the cyclohexane solution lead to decreasing relative amounts of I₃⁻ and increasing relative amounts of I⁻ to be released (Figure 4c,d).

It is not yet clear where the processes take place (inside the cavities, on the anions' surfaces, or both). The trapping process seems to be reversible up to a loading with 4 equiv of I₂, which might be indicative of a mere surface interaction. However, a loading with up to 11 equiv of I₂ is possible, as quantified by means of energy-dispersive X-ray (EDX) analysis, thermogravimetric analysis (TGA), and mass increase investigations, but

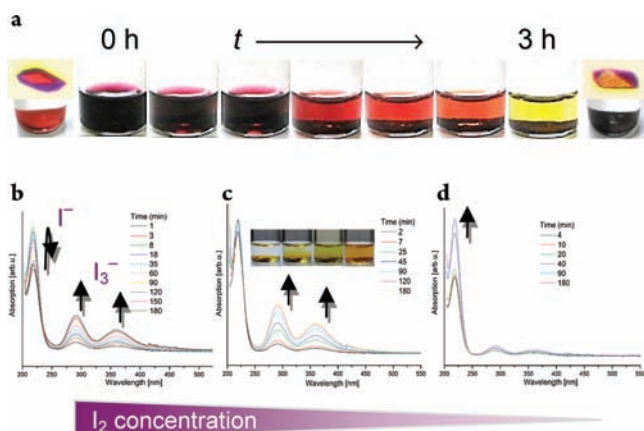


Figure 4. (a) Color change during a 3 h immersion of a 12.5 mg sample of ZBT-1 in 0.5 mL of an I_2 solution (0.05 mol/L) in cyclohexane. The photographs on the extreme left and extreme right illustrate the forms and colors of single crystals of ZBT-1 and ZBT-1-11 I_2 , respectively, together with photographs of the respective batches under pure cyclohexane. (b–d) Monitoring of the amount of released I^- ($\lambda_{max} = 218$ nm) and I_3^- ($\lambda_{max} = 290, 360$ nm) while soaking ZBT-1- nI_2 in ethanol for 3 h, using time-dependent UV-vis spectra. ZBT-1- nI_2 was formed during a 3 h treatment of ZBT-1 with excess I_2 in cyclohexane solution: (b) 40-fold excess ($n = 11$); (c) 25-fold excess ($n = 6$); (d) 18-fold excess ($n = 4$). The inset shows the ongoing color change.

also seems to affect the compound irreversibly (Table S2 and Figure S12). The fact that liquor is required for the bond cleavage indicates that this requires a higher mobility of the counterions, and thus rather takes place inside the “zeoballs”. Control experiments showed that neither K_2Se nor the precursor $[K_4(H_2O)_3][Ge_4Se_{10}]$ exhibits the same effect as ZBT-1. As verified by EDX analyses of crystals upon soaking, the I^+ ions do not stay at or within the anions; besides recombination with I^- ,²² they preferentially form IO^- , which immediately undergoes disproportionation reactions, as is known for this species in ROH solution.²³

In conclusion, an unprecedented molecular variant of a compound with zeolite-related composition has been achieved by employing ionothermal methods to chalcogenidotetrelate precursors, opening up an exciting new direction in the future development of chalcogenide compounds with extraordinary structural and functional properties.

■ ASSOCIATED CONTENT

📄 Supporting Information

Experimental procedures; SEM images; ESI-MS, EDX, and powder XRD data; details of X-ray structure refinement, TGA, UV-vis, and Raman measurements; and CIFs for ZBT-1 and ZBT-2. This material is available free of charge via the Internet at <http://pubs.acs.org>.

■ AUTHOR INFORMATION

Corresponding Author

dehnen@chemie.uni-marburg.de

Notes

The authors declare no competing financial interest.

■ ACKNOWLEDGMENTS

This work was supported by the Alexander von Humboldt Foundation and the Deutsche Forschungsgemeinschaft (DFG). We thank R. Riedel for X-ray data collection.

■ REFERENCES

- (1) Davis, M. E. *Nature* **2002**, *417*, 813.
- (2) (a) Chakrabarty, R.; Mukherjee, P. S.; Stang, P. J. *Chem. Rev.* **2011**, *111*, 6810. (b) Yu, J.; Xu, R. *Acc. Chem. Res.* **2010**, *43*, 1195. (c) Yang, H.-B.; Hawkrigge, A. M.; Huang, S. D.; Das, N.; Bunge, S. D.; Muddiman, D. C.; Stang, P. J. *J. Am. Chem. Soc.* **2007**, *129*, 2120.
- (3) Phan, A.; Doonan, C. J.; Uribe-Romo, F. J.; Knobler, C. B.; O’Keeffe, M.; Yaghi, O. M. *Acc. Chem. Res.* **2010**, *43*, 58.
- (4) (a) Feng, P.; Bu, X.; Zheng, N. *Acc. Chem. Res.* **2005**, *38*, 293. (b) Zheng, N.; Bu, X.; Wang, B.; Feng, P. *Science* **2002**, *298*, 2366. (c) Zheng, N.; Bu, X.; Feng, P. *Nature* **2003**, *426*, 428. (d) Zheng, N.; Bu, X.; Feng, P. *Angew. Chem., Int. Ed.* **2005**, *44*, 5299.
- (5) Ding, N.; Kanatzidis, M. G. *Nat. Chem.* **2010**, *2*, 187.
- (6) Cooper, E. R.; Andrews, C. D.; Wheatley, P. S.; Webb, P. B.; Wormald, P.; Morris, R. E. *Nature* **2004**, *430*, 1012.
- (7) Lin, Z.; Wragg, D. S.; Warren, J. E.; Morris, R. E. *J. Am. Chem. Soc.* **2007**, *129*, 10334.
- (8) Guloy, A. M.; Ramlau, R.; Tang, Z.; Schnelle, W.; Baitinger, M.; Grin, Y. *Nature* **2006**, *443*, 320.
- (9) (a) Zhang, Q.; Chung, L.; Jang, J. I.; Ketterson, J. B.; Kanatzidis, M. G. *J. Am. Chem. Soc.* **2009**, *131*, 9896. (b) Biswas, K.; Zhang, Q.; Chung, L.; Song, J.-H.; Androulakis, J.; Freeman, A. J.; Kanatzidis, M. G. *J. Am. Chem. Soc.* **2010**, *132*, 14760. (c) Li, J.-R.; Xie, Z.-L.; He, X.-W.; Li, L.-H.; Huang, X.-Y. *Angew. Chem., Int. Ed.* **2011**, *50*, 11395.
- (10) Dehnen, S.; Melullis, M. *Coord. Chem. Rev.* **2007**, *251*, 1259.
- (11) Lin, Y.; Dehnen, S. *Inorg. Chem.* **2011**, *50*, 7913.
- (12) Sheldrick, W. S.; Wachhold, M. *Coord. Chem. Rev.* **1998**, *176*, 211.
- (13) Kong, X.-J.; Long, L.-S.; Zheng, Z.; Huang, R.-B.; Zheng, L.-S. *Acc. Chem. Res.* **2010**, *43*, 201.
- (14) Wang, B.; Côté, A. P.; Furukawa, H.; O’Keeffe, M.; Yaghi, O. M. *Nature* **2008**, *453*, 207.
- (15) Li, H.; Laine, A.; O’Keeffe, M.; Yaghi, O. M. *Science* **1999**, *283*, 1145.
- (16) Wu, T.; Wang, L.; Bu, X.; Chau, V.; Feng, P. *J. Am. Chem. Soc.* **2010**, *132*, 10823.
- (17) Trikalitis, P. N.; Rangan, K. K.; Kanatzidis, M. G. *J. Am. Chem. Soc.* **2002**, *124*, 2604 and references therein.
- (18) Xu, R.; Zheng, W.; Guan, J.; Xu, Y.; Wang, L.; Ma, H.; Tian, Z.; Han, X.; Lin, L.; Bao, X. *Chem.—Eur. J.* **2009**, *15*, 5348.
- (19) (a) Chen, N.; Ortiz, A. L.; Echegoyen, L. In *Fullerenes: Principles and Applications*, 2nd ed.; Langa De La Puente, F., Nierengarten, J.-F., Eds.; Royal Society of Chemistry: Cambridge, U.K., 2011; pp 12–65. (b) O’Leary, B. M.; Szabo, T.; Svenstrup, N.; Schalley, C. A.; Lützen, A.; Schäfer, M.; Rebek, J., Jr. *J. Am. Chem. Soc.* **2001**, *123*, 11519. (c) Heinz, T.; Rudkevich, D. M.; Rebek, J., Jr. *Nature* **1998**, *394*, 764. (d) Schäfer, C.; Todea, A. M.; Gouzerh, P.; Müller, A. *Chem. Commun.* **2012**, *48*, 350.
- (20) (a) O’Regan, B.; Grätzel, M. *Nature* **1991**, *353*, 737. (b) Law, M.; Greene, L. E.; Johnson, J. C.; Saykally, R.; Yang, P. *Nat. Mater.* **2005**, *4*, 455.
- (21) (a) Zeng, M.-H.; Wang, Q.-X.; Tan, Y.-X.; Hu, S.; Zhao, H.-X.; Long, L.-S.; Kurmoo, M. *J. Am. Chem. Soc.* **2010**, *132*, 2561. (b) Abrahams, B. F.; Moylan, M.; Orchard, S. D.; Robson, R. *Angew. Chem., Int. Ed.* **2003**, *42*, 1848. (c) Choi, H. J.; Suh, M. P. *J. Am. Chem. Soc.* **2004**, *126*, 15844.
- (22) Kebede, Z.; Lindquist, S.-E. *Sol. Energy Mater. Sol. Cells* **1999**, *57*, 259.
- (23) Housecroft, C. E.; Sharpe, A. G. *Inorganic Chemistry*, 3rd ed.; Prentice Hall: London, 2008; Chapter 17.